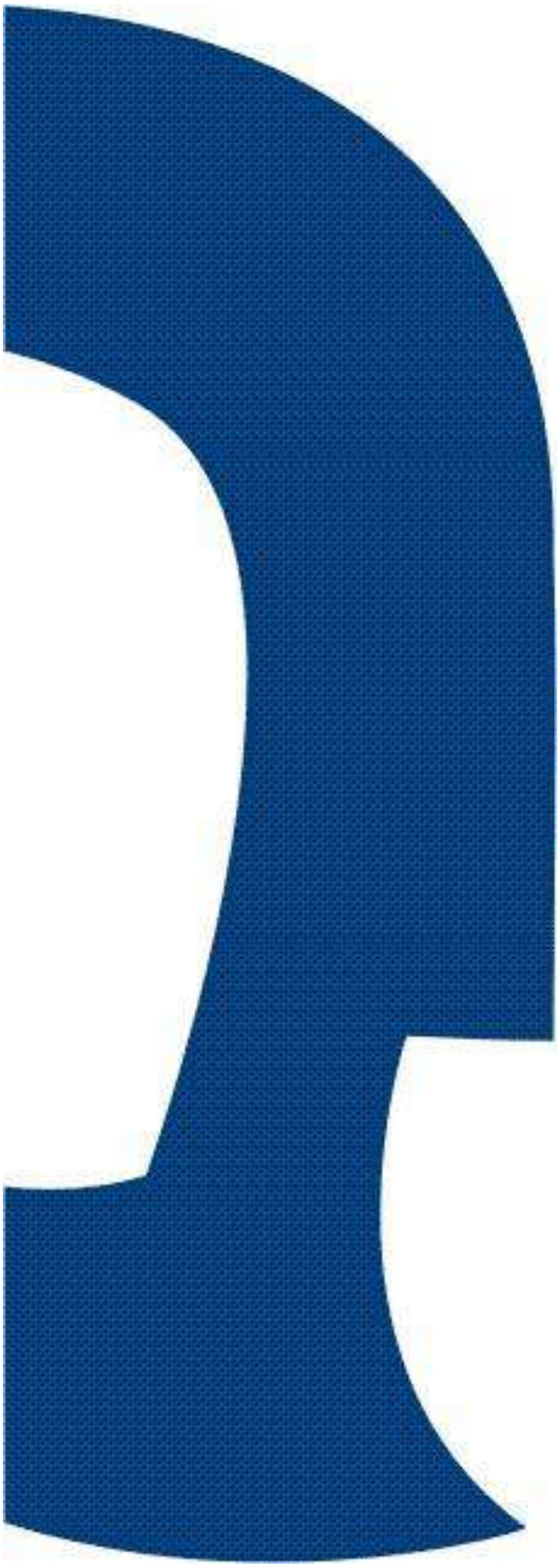

FACULTAD
DE CIENCIAS
DEL MAR

UNIVERSIDAD DE LAS PALMAS
DE GRAN CANARIA

Conceptual model for Sea-Breeze development in Fuerteventura

Cristian Alexis García Suárez

2019/2020

Luis Cesáreo Cana Cascallar
David Suárez Molina

Trabajo Fin de Título para la obtención del título Grado Ciencias del Mar

Title of TFG

Conceptual model for See-Breeze development in Fuerteventura

Personal information of the student

Name: Cristian Alexis García Suárez.

DNI: 51152011B

Degree: Grado Ciencias del Mar.

E-mail: cristian.garcia108@alu.ulpgc.es

Phone: 630881304

Information of the tutor and cotutor

Tutor: Luis Cesáreo Cana Cascallar. Profesor Departamento de Física. Facultad Ciencias del Mar. Universidad de Las Palmas de Gran Canaria.

E-mail: Luis.cana@ulpgc.es

Cotutor: David Suárez Molina. Técnico Superior de Meteorología (Agencia Estatal de Meteorología).

E-mail: dsuarezm@aemet.es

Date and signature of the student, tutor and cotutor

Firmado por SUAREZ MOLINA DAVID - 78511093H el día 18/09/2020 con un certificado emitido por AC FNMT Usuarios

CANA
CASCALLAR LUIS
CESAREO -
51659203F

Firmado digitalmente por
CANA CASCALLAR LUIS
CESAREO - 51659203F
Fecha: 2020.09.18
09:30:07 +01'00'

Cristian

INDEX

Abstract

The sea breeze is a mesoscale phenomenon that occurs in all coastal areas around the world. In the present study, it is analysed in the Canary archipelago, specifically in the island of Fuerteventura. This region is located in the North Atlantic Ocean, near the African continent, in the subtropical zone. The aim is to develop a conceptual model of the sea breezes in this island. To achieve this objective, the database of the state meteorological agency (AEMET) was used to observe the weather of Fuerteventura in the six stations spread over the island. The HRES-IFS model was also used to analyse the synoptic environment of the Canary Islands area and for simulated soundings. The WRF model was used to forecast meteorological variables at different altitudes and for vertical cross sections. In addition, satellite images from the MSG of the HRVIS channel were used to observe the clouds that form in the passage of the sea breeze. To describe the evolution of the sea breeze, two specific days will be studied in which there were strong breezes that entered to the central areas of the island, these days are 18 March 2017 and 5 April 2020. From these days, it has been concluded that the sea breeze in Fuerteventura is produced by a change in the wind direction from a NE component (trade winds) to a maritime component (SE component) that depends on synoptic conditions. Furthermore, there must be a minimum temperature difference of at least 2º C between sea and land to originate the movement of air from the ocean to inland. As result, two breeze circulations are formed at the same time, a breeze circulation to windward, the most studied, and another breeze circulation occurs to leeward. With all the results obtained, it has been possible to create a conceptual model of sea breeze in Fuerteventura at temporal and spatial scales to improve the knowledge of this phenomenon in the chosen area.

1. Introduction

1.1. Sea-Breeze concept

The sea breeze is a mesoscale phenomenon, a local circulation that occurs in coastal areas around the world, from the Polar Regions to the Equator (Miller et al. 2003). This phenomenon occurs under relatively cloudless skies (Miller et al. 2003) and begins during the morning, a few hours after sunrise, usually between 0900 to 1100 UTC, when solar radiation heats the earth's surface (Crosman and Horel 2010). Because the land and the ocean heat up at different rates, a temperature contrast is created between the two air masses, as the land heats up faster than the ocean. This thermal contrast creates a pressure gradient on a local scale causing a small area of low pressure on land. The air rises as the land warms it up and the colder air above the sea surface forms a high-pressure zone that causes this air mass to tend to occupy the space left by the warmer air that has risen above the land. Therefore, the mass of air at high-pressure over the ocean always tends to move towards the low-pressure zone above the land. This displacement creates the Sea Breeze Front (SBF), a cool front of between 300-1000 m in the vertical dimension (Crosman and Horel 2010).This front, when penetrating inland, forms a general low-level convergence in its vicinity inducing upward current air movement. When there is sufficient humidity, this upward current can extend along the entire coast forming a continuous line of low-level clouds parallel to the coast that can move a couple of kilometres inland, which can be used to locate the SBF using satellite images (Crosman and Horel 2010; Ferdiansyah et al. 2020) as it is shown in (Fig. 1a). In addition, due to this pressure gradient, a return current is created that is approximately twice as thick as the SBF so that the total vertical dimension of the sea breeze ranges from 1 to 3 km (Crosman and Horel 2010). And there is a return current that close the cycle through the subsidence, thus forming the circulation of the sea breeze (Fig. 1b).

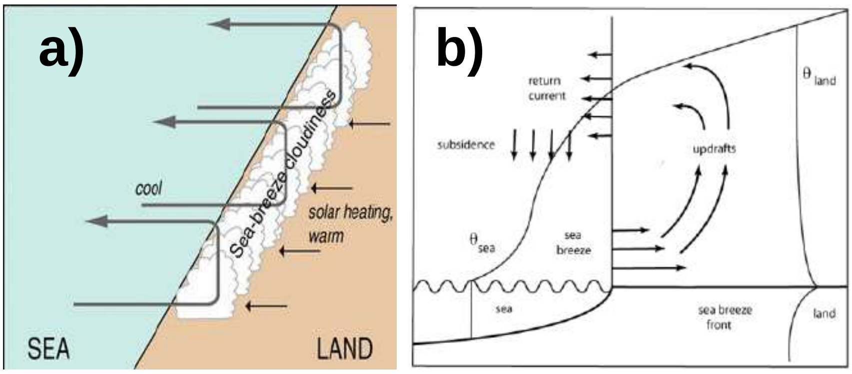

Fig. 1 The diagrams above show a sea breeze circulation. **a)** This scheme shows the thermal contrast between sea (cool) and land (warm) and the sea-breeze cloudiness **b)** This image presents all horizontal and vertical processes (EUMeTrain 2020).

It should be noted that the formation of the sea breeze depends not only on the distance from the coast, but also on spatial variations in topography, land surface properties and synoptic conditions (Ferdiansyah et al. 2020).

For the measurement and classification of the spatial and temporal dimensions of meteorological phenomena, the most widely used scale is that of Orlanski (1975), which divides phenomena according to their extent and duration into micro-scale (e.g. a whirlwind), mesoscale (a storm) and macro-scale (long waves), from smaller to larger scale respectively. The sea breeze is a mesoscale-β phenomenon, where the sea breeze has horizontal dimension of 30 km and a life cycle about 10 hours approximately. The sea breeze begins between 0900-1000 UTC with daytime warming, has a maximum advance around 1300 UTC, retreats from this time and disappears completely around 1900 UTC. (Fig. 2) (Orlanski 1975; Lin 2007; AEMET 2020a).

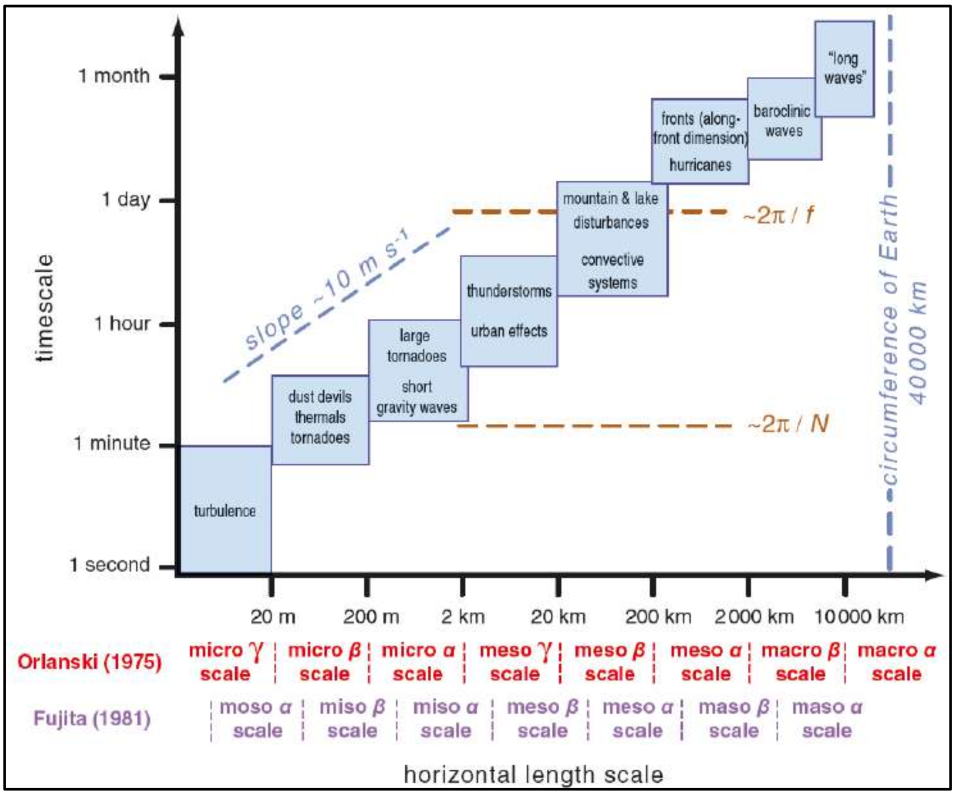

Fig. 2 Meteorological scales according to their extensions and duration with the Orlanski and Fujita classification (AEMET 2020a).

In order to understand the physical basis behind the formation of this mesoscale phenomenon, it must be taken into account that this phenomenon originates in accordance with the circulation theorem for a baroclinic fluid (Holton and Hakim 2004), which is characterized by the fact that the isobaric and isopycnic surfaces are not parallel. In this study, a rate of lagrangian change of the absolute circulation was used, obtaining:

$$\frac{DC_a}{Dt} = \frac{D}{Dt}\oint U_a \cdot dl = -\oint \rho^{-1} dp \qquad (1.1)$$

This process can be illustrated by considering the case of the sea breeze, as it can be seen in Fig. 3:

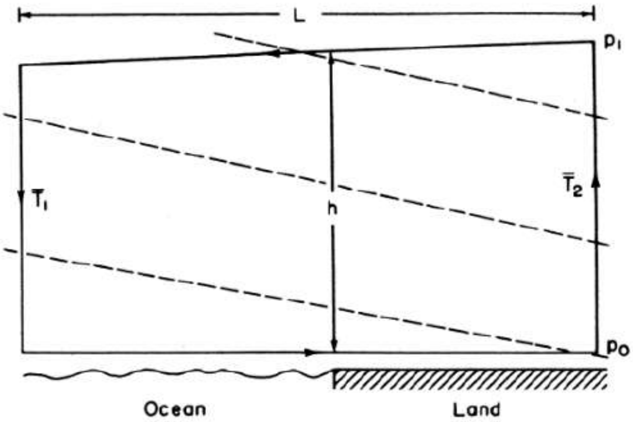

Fig. 3 Application of the circulation theorem to the sea breeze problem. The closed heavy solid line is the loop about which the circulation is to be evaluated. Dashed lines indicate surfaces of constant density (Holton and Hakim 2004).

For this situation, the average temperature in the air above the ocean is colder than the average temperature on the adjacent land. Therefore, that thermal contrast causes that the isobaric surfaces (surfaces of constant pressure) on the ground will gravitate towards the ocean while the isopycnic surfaces (surfaces of constant density) will gravitate towards the land. To calculate the acceleration as a result of the intersection of pressure-density surfaces, we apply the circulation theorem by integrating around a circuit in a vertical plane perpendicular to the coastline. Substituting the law of ideal gases in (1.1), we obtain:

$$\frac{DC_a}{Dt} = -\oint R\,T\,d\ln p \qquad (1.2)$$

In the circuit shown in figure 2, there is a contribution to the line-integral only for the vertical segments of the loop, since the horizontal segments are taken at constant pressure. The resulting rate of increase in circulation is:

$$\frac{DC_a}{Dt} = R\ln\left(\frac{p_0}{p_1}\right)(\overline{T_2} - \overline{T_1}) > 0 \qquad (1.3)$$

By leaving (ϑ) the average tangential speed along the circuit, we obtain:

$$\frac{D\vartheta}{Dt} = \frac{R\ln(p_0/p_1)}{2(h+L)}(\overline{T_2} - \overline{T_1}) \qquad (1.4)$$

With this formula it can be said that as wind speed increases, frictional force reduces the rate of acceleration and temperature advection reduces the land-sea temperature contrast so that a balance is obtained between the generation of kinetic energy by pressure-density solenoids and frictional dissipation (Holton and Hakim 2004).

1.2. Objective

The aim of this study is to create a conceptual model of sea breeze for Fuerteventura, in order to improve the knowledge of this meteorological phenomenon on the island. This work is novel because there is not a conceptual model of sea breeze in this island.

2. Methodology

The methodology followed for this study is, on the one hand, the search for specific days when sea breeze occurs, in this case, for 18 March 2017 and 5 April 2020. These days have been chosen because there were intense breezes that affected even the central areas of the island. In addition, each event presents singularities that will be explained in more detail later. On the other hand, the interpretation of the results obtained will be conducted to conclude with the aim of creating a conceptual model of sea breeze in Fuerteventura which, according to (ZAMG 2020): "a conceptual model describes the essential features of a meteorological phenomenon and identifies the principal processes taking place".

These conceptual models have been described, for the first time, at the beginning of the 1990s and, to date, around 80 have been identified and described in various literatures. For example, in 1996, the "Manual of Synoptic Satellite Meteorology-Conceptual Models" was the start of this type of study by the Austrian Meteorological Institute (ZAMG) and has become an important diagnostic tool, widely used by meteorological services (EUMETSAT 2020). Therefore, the methodology followed to carry out the conceptual model in this work has been achieved by following a series of points that set out what a complete conceptual model must have (ZAMG 2020):

- Definition of the phenomenon in terms of features recognizable by observations, analysis, or validated simulations.
- Description of its life cycle in terms of appearance, size, intensity and accompanying weather.
- Statement of the controlling physical processes which enables the understanding of the factors that determine the mode and rate of evolution of the phenomenon.
- Specification of the key meteorological fields demonstrating the main processes.
- Guidance for predicted meteorological conditions or situations using the diagnostic and prognostic fields that best discriminate between development or non-development; guidance for predicting displacement and evolution.

With the contributions made in this study, all the points mentioned above have been achieved and thus the objective of this study.

2.1. Study area

2.1.1. Location

The study area is located in the Canary Islands, more precisely in the island of Fuerteventura (red box in Fig. 4a), this archipelago is composed of seven islands that are in the North Atlantic, west of the African continent, covering from 27°37′ to 29°25′N and from 18°10′ to 13°20′W, therefore, all the islands are in the subtropical zone (Suárez Molina et al. 2020). For the analysis of the meteorological situation on the studied island, the data from the six automatic weather stations (Fig. 4b) coming from the AEMET database distributed on this island will be collected and interpreted.

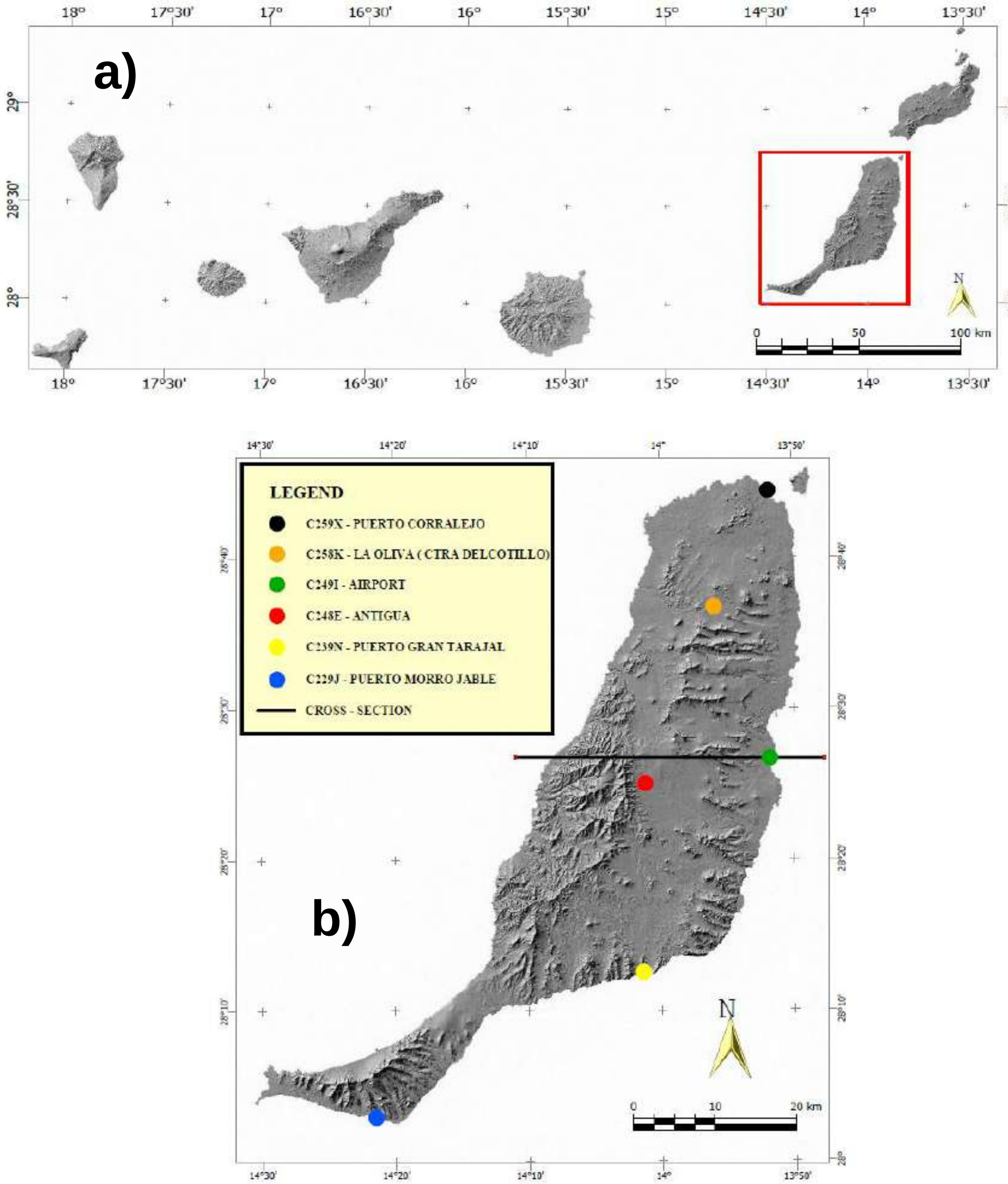

Fig. 4 **a)** Location of the study area within in the Canary Islands. **b)** Location of the six AEMET stations and the cross-section in the island of Fuerteventura.

2.1.2. Climatology

The area of the Canary Islands is governed by the presence of the descending branch of the Hadley cell around 30º N, which establishes a generalized regime of subsidence in the free troposphere, the Canary current which brings cold water to all the islands from the north and the predominance of the trade winds. One of the most important features of the climate of this region is the persistence throughout the year of a vertical structure of the troposphere with frequent thermal inversions of the subsidence type, which gives a predominance of stability, resulting in fair weather (Dorta Antequera 1996; Carrillo et al. 2016; Suárez Molina et al. 2020).

It should be mentioned that, according to Köppen classification, there are different types of climate. In his classification, the island of Fuerteventura has a dry or B-type climate, where Köppen also distinguishes two subtypes of climate, BS (steppe) and BW (desert) according to annual rainfall. It also distinguishes between hot (letter h) and cold (letter k) varieties depending on whether the average annual temperature is above or below 18° C, respectively. Therefore, Fuerteventura has a predominantly BWh type climate (García Couto 2012).

A climatological survey of Fuerteventura airport is shown in Fig. 5, with a reference period from 1981 to 2010, where the variables are shown: temperature (average, average max. and min., max. and min. absolute) in º C, precipitation (average, max. 24 h and Nº of days) in mm, average Nº of days with presence of snow, storm and frost and Hours of sunlight for each month of the year (AEMET 2018):

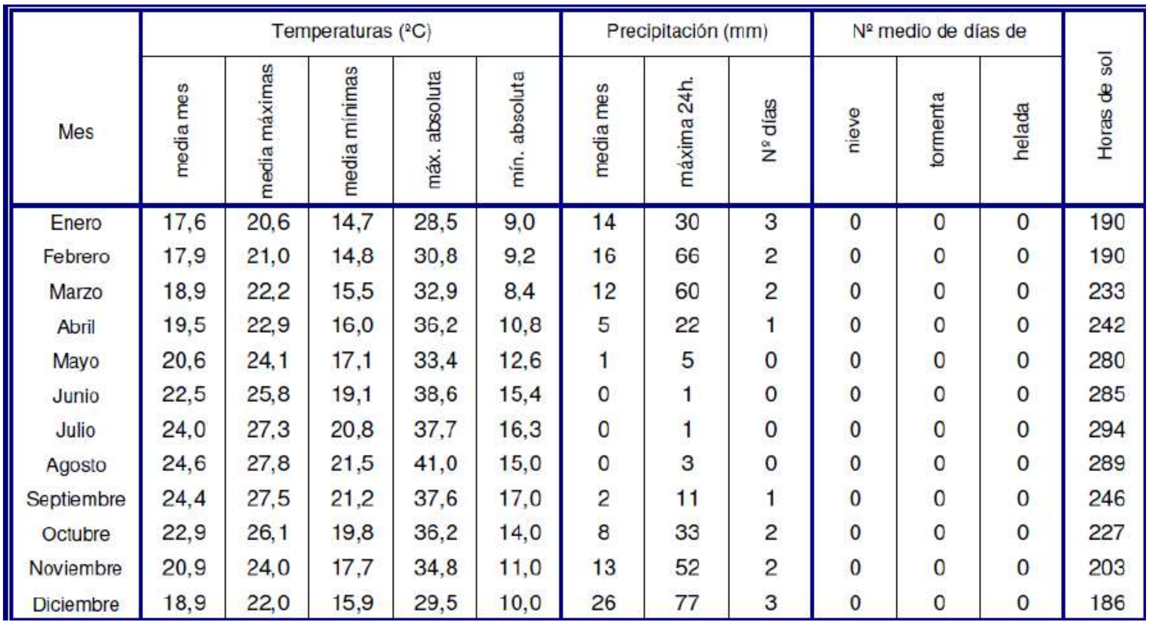

Mes	Temperaturas (ºC)					Precipitación (mm)			Nº medio de días de			Horas de sol
	media mes	media máximas	media mínimas	máx. absoluta	mín. absoluta	media mes	máxima 24h.	Nº días	nieve	tormenta	helada	
Enero	17,6	20,6	14,7	28,5	9,0	14	30	3	0	0	0	190
Febrero	17,9	21,0	14,8	30,8	9,2	16	66	2	0	0	0	190
Marzo	18,9	22,2	15,5	32,9	8,4	12	60	2	0	0	0	233
Abril	19,5	22,9	16,0	36,2	10,8	5	22	1	0	0	0	242
Mayo	20,6	24,1	17,1	33,4	12,6	1	5	0	0	0	0	280
Junio	22,5	25,8	19,1	38,6	15,4	0	1	0	0	0	0	285
Julio	24,0	27,3	20,8	37,7	16,3	0	1	0	0	0	0	294
Agosto	24,6	27,8	21,5	41,0	15,0	0	3	0	0	0	0	289
Septiembre	24,4	27,5	21,2	37,6	17,0	2	11	1	0	0	0	246
Octubre	22,9	26,1	19,8	36,2	14,0	8	33	2	0	0	0	227
Noviembre	20,9	24,0	17,7	34,8	11,0	13	52	2	0	0	0	203
Diciembre	18,9	22,0	15,9	29,5	10,0	26	77	3	0	0	0	186

Fig. 5 Weather summary of Fuerteventura airport showing different temperatures (º C) and precipitations (mm), mean number of days with snow, storm and frost and hours of sun for each month from 1981 to 2010 (AEMET 2018).

In addition, a clear difference between summer and winter can be seen in Fig. 5, where the island of Fuerteventura at the altitude of the airport presents an average temperature of 24º C in summer and 18º C in winter rainfall can also be seen during the winter months and less in the adjacent months, while in the summer months there is hardly any rainfall on this island and, due to the location of the study area, there are no days of snow, storm or frost.

To study the probability of sea breeze in Fuerteventura, the frequency of wind speed and direction at Fuerteventura airport will be observed throughout March and April. It has been observed that the two months show fairly similar results therefore only the March results will be shown.

For March there is a reference period from 2002 to 2016, with a number of observations of 16162 (0000 to 2300 UTC). The wind direction is shown in sectors of 30º and the wind speed in intervals of 5 knots (Fig. 6):

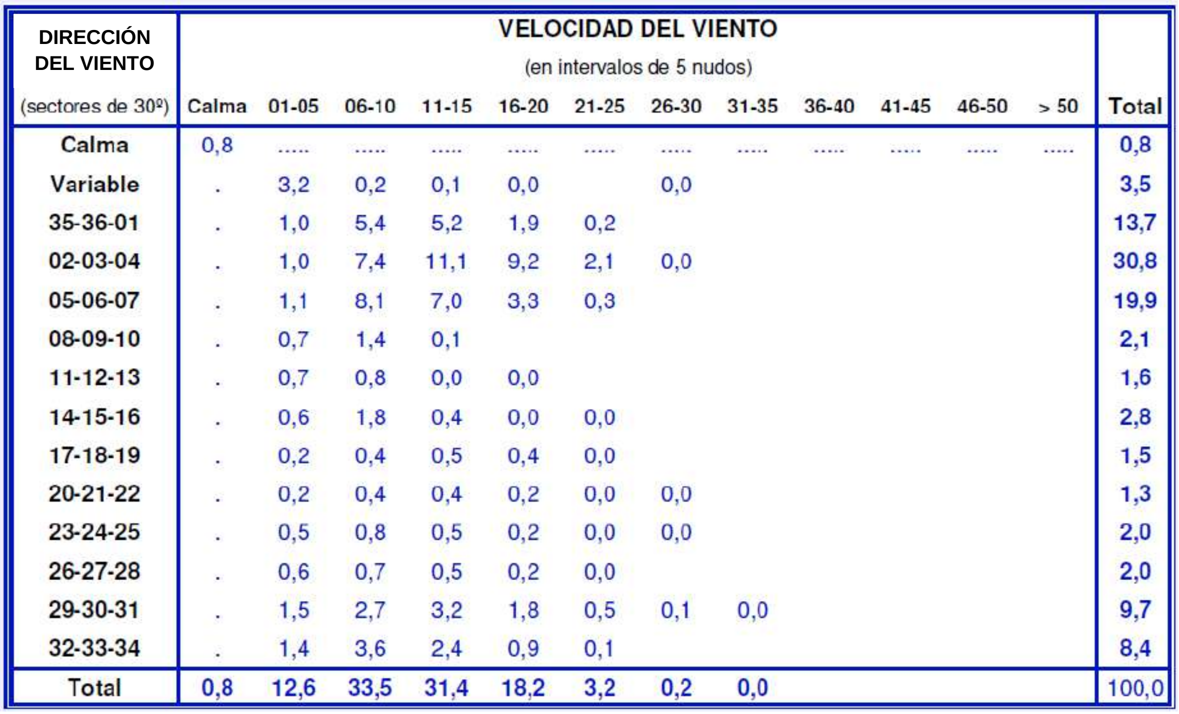

DIRECCIÓN DEL VIENTO	VELOCIDAD DEL VIENTO (en intervalos de 5 nudos)												
(sectores de 30º)	Calma	01-05	06-10	11-15	16-20	21-25	26-30	31-35	36-40	41-45	46-50	> 50	Total
Calma	0,8	.....	.....	.....	.....	.....	.....	.....	.....	.....	.....	.....	0,8
Variable	.	3,2	0,2	0,1	0,0		0,0						3,5
35-36-01	.	1,0	5,4	5,2	1,9	0,2							13,7
02-03-04	.	1,0	7,4	11,1	9,2	2,1	0,0						30,8
05-06-07	.	1,1	8,1	7,0	3,3	0,3							19,9
08-09-10	.	0,7	1,4	0,1									2,1
11-12-13	.	0,7	0,8	0,0	0,0								1,6
14-15-16	.	0,6	1,8	0,4	0,0	0,0							2,8
17-18-19	.	0,2	0,4	0,5	0,4	0,0							1,5
20-21-22	.	0,2	0,4	0,4	0,2	0,0	0,0						1,3
23-24-25	.	0,5	0,8	0,5	0,2	0,0	0,0						2,0
26-27-28	.	0,6	0,7	0,5	0,2	0,0							2,0
29-30-31	.	1,5	2,7	3,2	1,8	0,5	0,1	0,0					9,7
32-33-34	.	1,4	3,6	2,4	0,9	0,1							8,4
Total	0,8	12,6	33,5	31,4	18,2	3,2	0,2	0,0					100,0

Fig. 6 Showing wind direction in 30 degree sectors and wind speed in 5 knot intervals with their frequency (AEMET 2018).

It can be observed in the red boxes (Fig. 6) that the dominant wind comes from sectors 02-03-04 and 05-06-07, which indicate a NE wind direction (Fig. 7a) and with a wind intensity between 6 - 15 kt, which correspond to the trade winds having a percentage of presence of 65% (Fig. 7b). On the other hand, in the blue box (Fig. 6), there is a wind coming from sectors 08-09-10, 11-12-13, 14-15-16 and 17-18-19, which are E-S component winds, which are of interest for this study and correspond to maritime component winds. These winds can be seen when the trade winds are not present, and it should be pointed out that winds with a maritime component show the highest percentage of presence when they are in the interval 1 - 5 kt with 17.5% of cases (Fig. 7c). In the other intervals such as, for example, the interval 6 - 10 kt, little presence of winds with a maritime component has been observed (Fig. 7d).

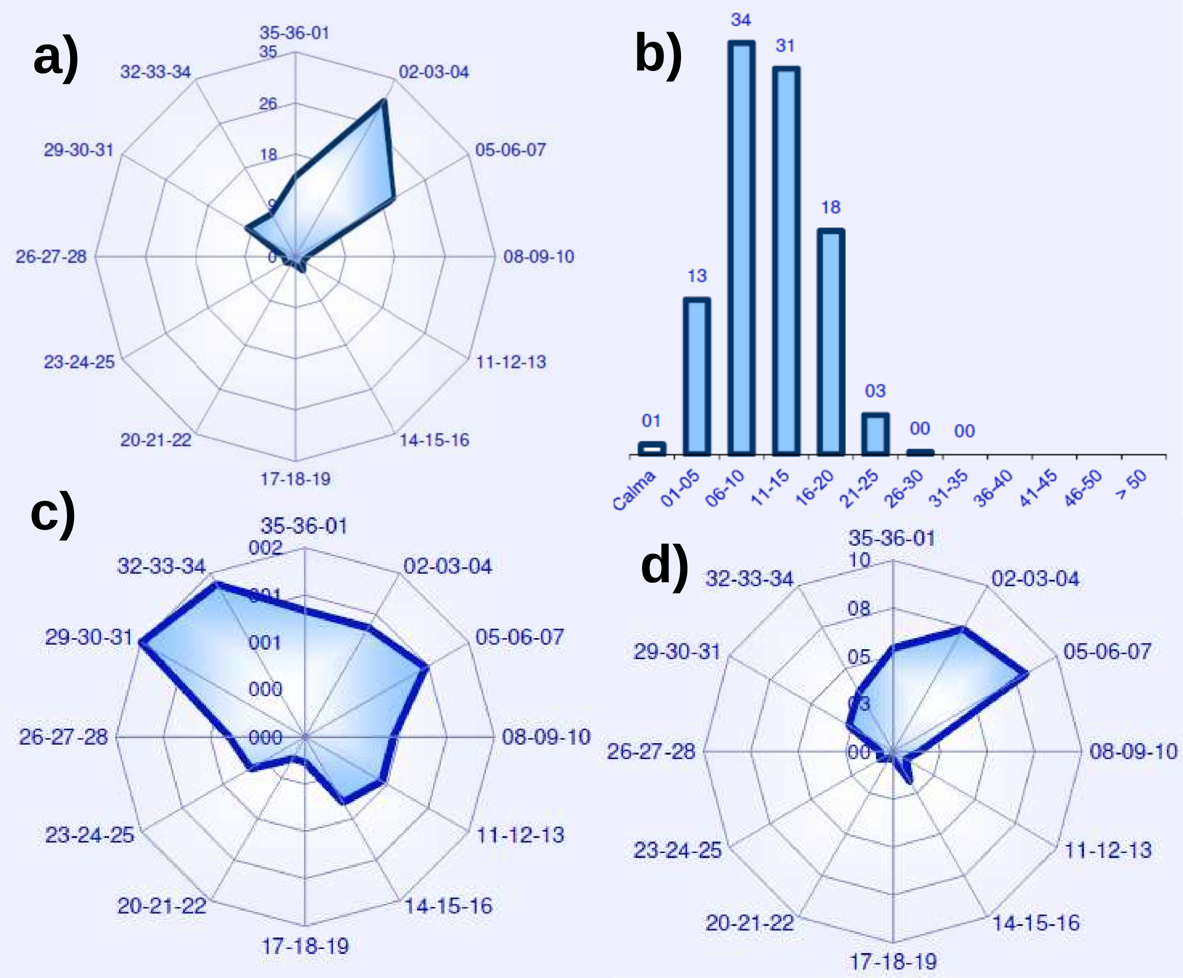

Fig. 7 **a)** Wind rose for all winds. **b)** Frequency of wind speed for all winds. **c)** Wind rose for winds in the interval 1-5 kt. **d)** Wind rose for winds in the interval 6-10 kt (AEMET 2018)**.**

2.2. Data

The data used for the results are extracted as time-series from AEMET database, as maps for the reanalysis data with HRES-IFS model (High Resolution Integrated Forecast System) coming from the ECMWF (European Centre for Medium-Range Weather Forecasts), as maps for WRF (Weather Research and Forecasting) data, where the Boundary Conditions (BCs) have been provided by UCAR (University Corporation for Atmospheric Research) and as images for satellite data coming from Meteosat Second Generation (MSG) with the HRVIS (High-Resolution Visible Imaging System) channel.

2.2.1. AEMET database

As for the time series obtained from the AEMET database, they have a ten-minute resolution and, as an objective, observe the behavior of the meteorological variables wind direction, wind speed, temperature and precipitation at each of the stations in the island of Fuerteventura (Fig. 5b). Furthermore, this type of graphics provides us with numerical data such as total precipitation, minimum and maximum temperature, maximum wind gust and lightning count. It should be mentioned that the terminology used is in accordance with the current Manual of Uses of Meteorological Terms (AEMET 2015).

2.2.2. HRES-IFS Model

The aim of the HRES-IFS model maps is to analyze the synoptic environment of the Canary Islands area. Two synoptic maps have been used, one showing the geopotential next to the temperature at 500 hPa and another map shows the pressure at sea level with temperature at 850 hPa. Moreover, this model has been used to create simulated soundings in the island of Fuerteventura to observe the vertical profile of several meteorological variables in the atmosphere. It should be worth noting that this model has a resolution of 0.1º in latitude and longitude (approximately 10 km) and a range of 10 days or 240 hours (AEMET 2020b).

2.2.3. WRF Model

Two different outputs have been used for the WRF model maps, one showing wind at 10 m with temperature at 2 m and another showing wind speed at 10 m with wind module. These NCEP FNL (Final) operational global analysis and forecast data are on 0.25-degree by 0.25-degree grids prepared operationally every six hours. This product is from the Global Data Assimilation System (GDAS) (Cana et al. 2020). In addition, this tool has been used to show vertical sections in the airport zone (Fig. 5b), one with the potential temperature (K) and vertical speed component (dPa s^{-1}) and another with the speed component perpendicular to the coast and the circulation vectors. More information on the configuration adopted in the simulations with the WRF model can be found in Cana et al. (2020).

2.2.4. MSG (HRVIS)

The satellite images coming from the MSG using the HRVIS channel, aim to observe what kind of cloud formation is present on the island. It should be noted that the HRVIS channel has been used because it has a higher spatial resolution than the IR (Thermal Infrared) and WV (Water Vapor) channels.

3. Results

This section will monitor the weather events on 18 March 2017 and 5 April 2020 using the tools set out in the Data section.

3.1. March 2017 event

The results obtained for the 18 March 2017 will be shown, where an episode of sea breeze with a low height occurred, which favored the convergence and provided rainfall on the island.

3.1.1. Meteorological stations

The meteorological stations of the airport (C249I) and the Carretera del Cotillo (C258K) have been chosen for this day from the six stations on Fuerteventura because they are located near the coast and inland respectively (Fig 4b). In addition, the airport station is the most important because it is situated in the flat area closest to the source of the sea breeze.

In the airport station (Fig. 8a), it can be seen the wind is generally light (average wind speed between 6 km/h and 20 km/h), during the night and part of the morning it is of N component and, during the afternoon, it is variable and turns to E and/or S component with a wind speed interval between 21 km/h and 40 km/h between 1600-1900 UTC, in which the maximum recorded gust of 42 km/h stands out, as shown in the orange box. The minimum temperature was 13º C and was recorded between 0700-0800 UTC, and the maximum was 20º C at 1200 UTC. Moreover, when the wind changes direction to an E and/or S component the temperature remains unchanged. Also 13 lightning were registered between 1300-1400 UTC and 1500-1700 UTC. From 1000 UTC with the diurnal warming the flow turned to marine component (SE component) giving rise to the phenomenon of sea breezes (red box).

In the Carretera del Cotillo station (Fig. 8b), it can be observed calm wind conditions during the night and weak during the day. Furthermore, during the day it was generally N component, but it turned to E and/or S component at 1400-1500 UTC. As for the temperature, the minimum was 11º C and it took place at 0700-0800 UTC, and the maximum was 20º C at 1500 UTC. It was also recorded one lightning between 1500-1600 UTC, and heavy rain between 1700-1900 UTC (blue box), with a total rainfall of 18.6 mm. As mentioned above, the flow turned to a maritime component in some time intervals, with a sea breeze phenomenon (red box) standing out among the 1500-1800 UTC in which precipitation occurred.

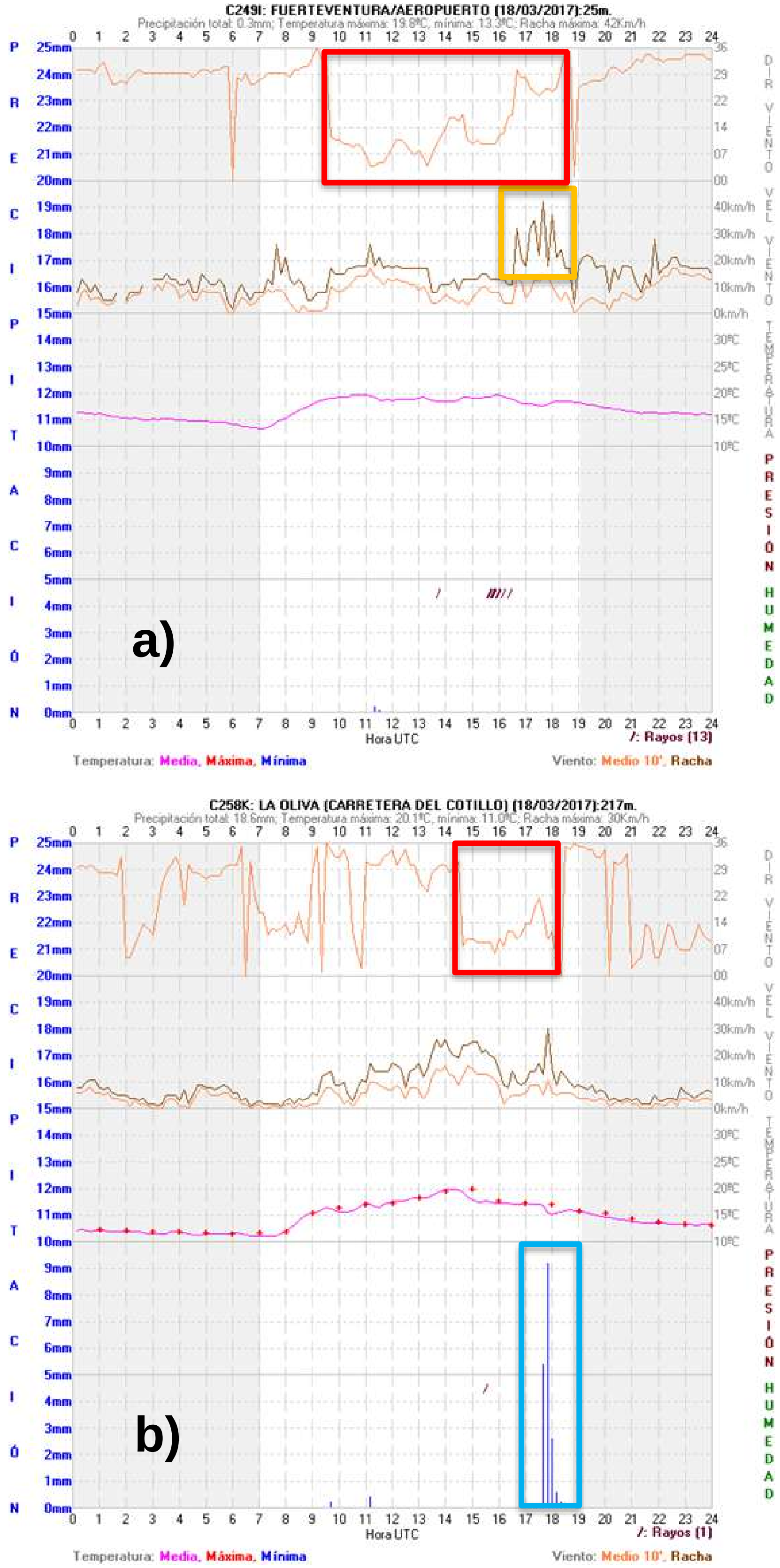

Fig. 8: 24 hour graphs for 18 March 2017 showing wind direction, wind speed (km / h), temperature (º C), precipitation (mm) and lightning count in the **a)** Airport station (C249I) and **b)** The Carretera del Cotillo station (C258K) (Source: AEMET).

As mentioned above, the six AEMET stations have been studied and two of them have been analyzed and exposed for this situation in this work. Likewise, to expose the situation in the other stations, the most important data from each station have been collected for 18 March 2017 (Table 1).

Table 1 Summary of the most important data for each station on 18 March 2017 showing the station code and name, the height of the station, minimum (TN) and maximum (TM) temperature, total precipitation (Prec), maximum gust of wind (RM), wind strength and the presence of sea breeze.

Station	Name	Height (m)	TN (º C)	TM (º C)	Prec (mm)	RM (km/h)	Wind strength	Breeze
C259X	**La Oliva-Pto**	**6**	**15.4**	**19.7**	**0**	**28**	**Weak**	**No**
C258K	**La Oliva-Ctra del Cotillo**	**217**	**11.0**	**20.1**	**18.6**	**30**	**Calm / Weak**	**Yes**
C249I	**Aeropuerto**	**25**	**13.3**	**19.8**	**0.3**	**42**	**Weak**	**Yes**
C248E	**Antigua-El Carbón**	**252**	**10.9**	**18.8**	**11.4**	**28**	**Weak**	**Yes**
C239N	**Tuineje-Pto**	**1**	**13.4**	**23.5**	**0.2**	**22**	**Weak**	**Yes**
C229J	**Pájara-Pto**	**15**	**16.5**	**30.1**	**0**	**23**	**Weak**	**Yes**

3.1.2. HRES-IFS Model

As for the outputs of the HRES-IFS model, the synoptic environment and a simulated sounding in Fuerteventura for 18 March 2017 have been studied.

Synoptic environment

In the synoptic environment for 18 March 2017, a cold core was observed at 500 hPa over the Canary Islands (Fig. 9a). Additionally, it can be seen that they are inside a barometric swamp and, in its vicinity, a low with a minimum pressure of 1012 hPa centered on the African continent (Fig. 9b).Therefore, the islands were affected by a surface S component flow.

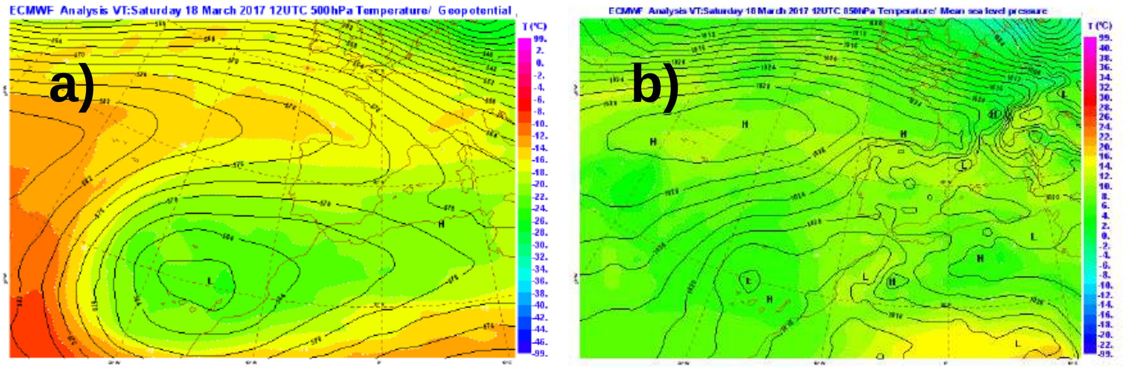

Fig. 9 Analysis from ECMWF model (18 March 2017 1200 UTC). **a)** 500 hPa temperature and geopotential. **b)** Mean sea level pressure and 850 hPa temperature (Source: AEMET).

Sounding

Nowadays, the increase in the spatial-temporal resolution of the numerical prediction models means that the predicted soundings are increasingly like the observed soundings (Suárez Molina et al. 2020). In this respect, a simulated sounding of the HRES-IFS model has been used to analyze the instability present over Fuerteventura (Fig. 10). The instability is very important to study because it explains the vertical displacement of the air parcels depending on the temperature difference between an air parcel and the surrounding air (AEMET 2020c).

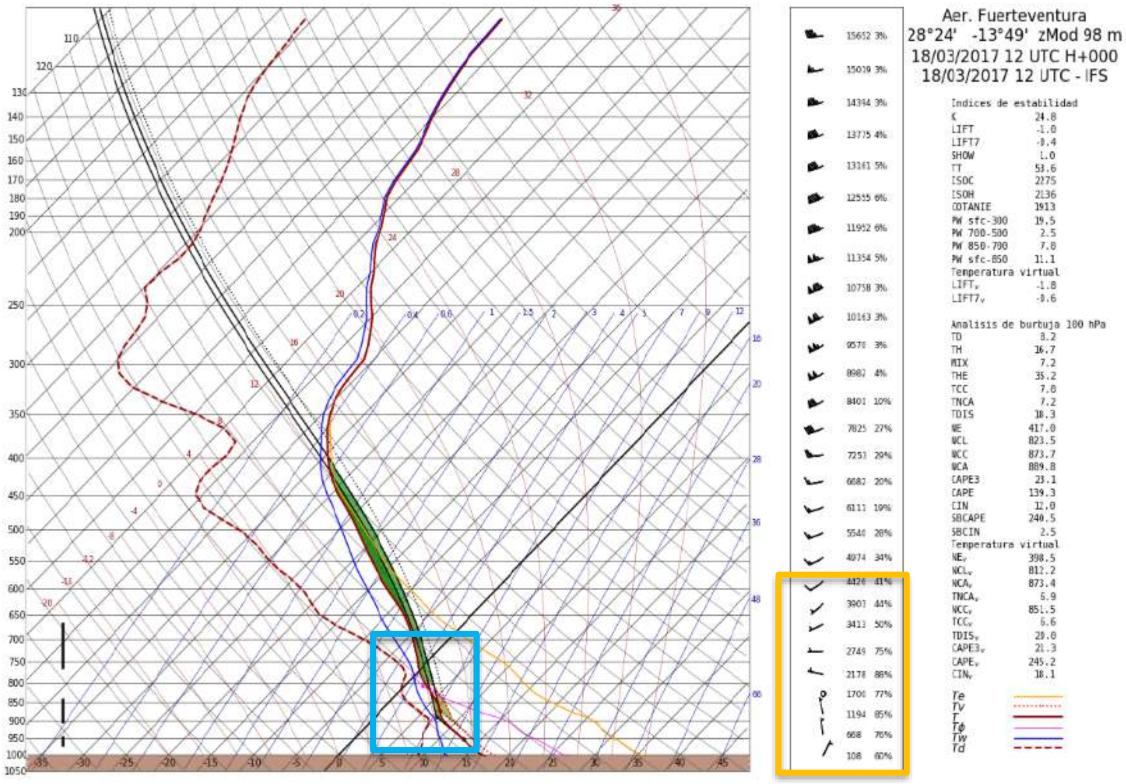

Fig. 10 Simulated sounding for 18 March 2017, 1200 UTC (Source: AEMET).

The simulated sounding at Fuerteventura airport at 1200 UTC for 18 March 2017 showed that the trade wind inversion was weak at 850 hPa. Therefore, the month of March has the lowest percentage of trade inversion with respect to the other months of the year at 68 % (Dorta Antequera 1996; Torres et al. 2001). It can be seen that there was a change of direction in the wind at 1700 m as it came from the N or NW and it changed of direction now coming from the W or SW as shown in the orange box. The LCL (Lifted Condensation Level) is approximately in 889 hPa as the T and Td approach and the air is more humid (blue box). In addition, a value of <20 and >30 in the K index is observed in the stability indices, indicating the possibility of a storm with heavy rainfall of between 20-60%, a negative value in the LIFT index favours instability and, therefore, the rise in air and a value of <50 and >55 in the TT index indicates a moderate probability of severe local storms (AMS 2012).

3.1.3. WRF Model

Regarding the outputs of the WRF model, this tool has been used to create two forecasts showing the evolution of different variables and to create vertical W-E sections across the airport station and which are also perpendicular to the coast (Fig. 4a).

WRF forecasts

Several WRF forecast have been studied for the 18 March 2017. One of them shows wind at 10 m with temperature at 2 m (Fig. 11a) and another shows wind speed at 10 m with wind module (Fig. 11b). For further detail, it has been observed that between 1300-1800 UTC a convergence is displayed inside the island as shown in the wind direction at 1300 UTC (Fig. 11a) and two fronts of the sea breeze are shown that are identified as white lines, one in the central area of the island and the other over Morro Jable (red box) also at 1300 UTC (Fig. 11b). In addition, it can be observed that two sea breeze cells are produced, one on the windward side, which has been studied in the stations, and the other on the leeward side.

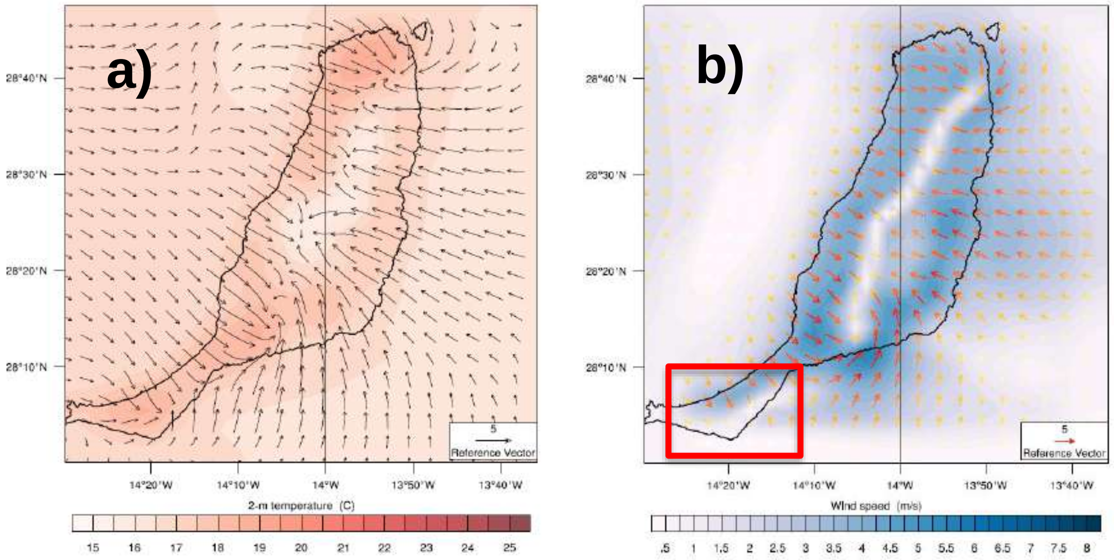

Fig. 11 WRF forecasts valid for 18 March 2017, 1300 UTC. **a)** 2-m temperature and 10-m wind speed (m s^{-1}) at dawn, **b)** 10-m wind speed (m s^{-1}) and wind module.

Cross-sections

The WRF model has been used to forecast the vertical structure of the sea breeze, representing a vertical section of W-E across the airport station, which is also perpendicular to the coast (Fig. 4a). The diagram on the left combines the potential temperature (K) and the vertical velocity component (dPa s^{-1}) to analyze the strong upward flow associated with the progression of the sea breeze (Fig. 12a), while the diagram on the right shows the perpendicular velocity component to the coast (m s^{-1})

where a red shaded area indicates an east-west flow. Besides, the circulation vectors are shown to determine the vertical structure of the flow and the extension of the sea breeze circulation cell (Fig. 12b) (Cana et al. 2020).

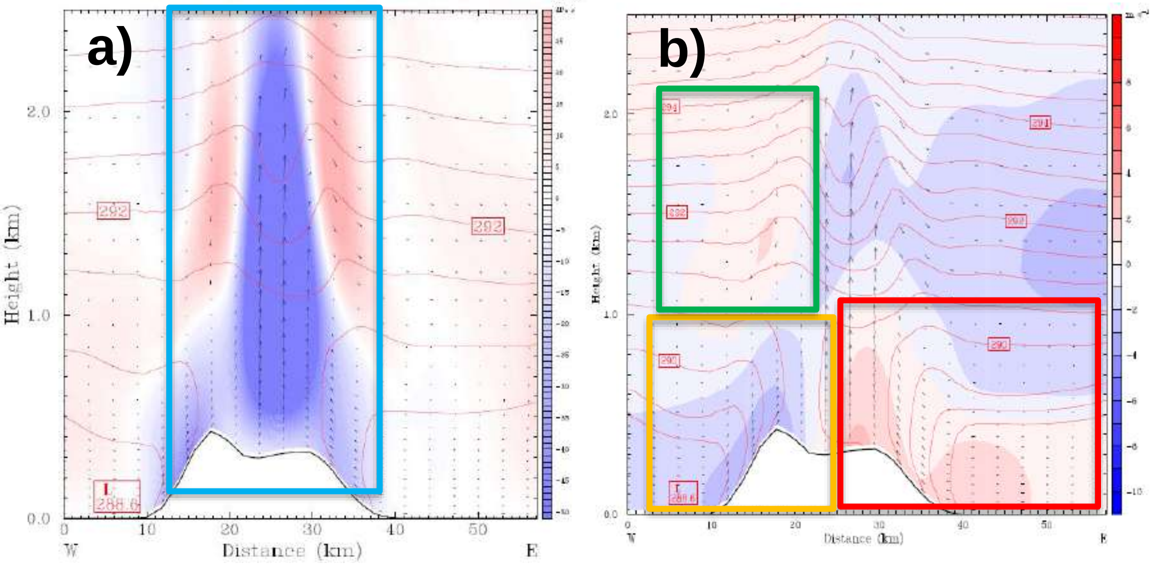

Fig. 12 Cross-section valid for 18 March 2017, 1400 UTC. **a)** Potential temperature (K) and vertical velocity component (dPa s^{-1}). **b)** Perpendicular velocity component to the coast (red contours denote movement from the east to the west) and circulation vectors. Source: (Cana et al. 2020).

For the situation in 18 March 2017, there was a significant vertical speed (blue zone) throughout the island where the vertical section has been made and which reached a height of more than 2 km as shown in the blue box (Fig. 12a). This was due to the cold core in height which favours the weakening of the trade wind inversion and, therefore, a strong convergence and a strong rise in the winds to higher layers. Moreover, the cell of the sea breeze, which is presented as winds from the east to the west, even reached the inland areas of the island as seen in the red box (Fig. 12b). It should be pointed out the existence of the other sea breeze that formed in favor of the general flow on the west coast of the island (orange box). This can be identified because there was a shallow return current, because it was in the opposite direction to the general flow (green box)(Cana et al. 2020).

3.1.4. Satellite images

For the observation of the cloudiness present on the island, satellite images of the MSG have been used with the HRVIS channel for 18 March 2017. A continuous line of clouds can be seen parallel to the east coast of the island of Fuerteventura as shown in the red box (Fig. 13), which reached the central areas of the island and can be used to identify the SBF and its evolution.

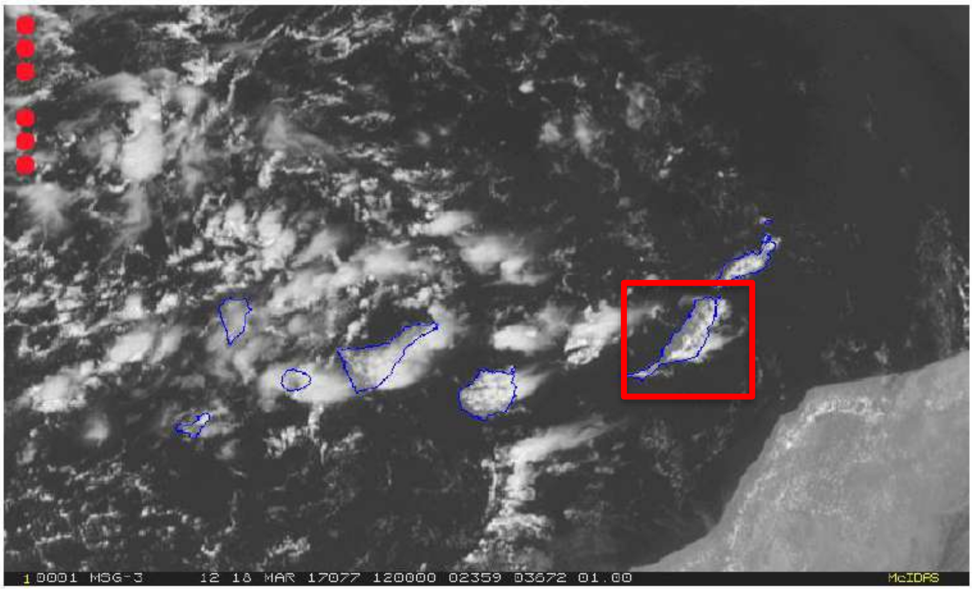

Fig. 13 Satellite image valid for 18 March 2017, 1200 UTC (Source: AEMET).

3.2. April 2020 event

In this subsection the results obtained for the 5 April 2020 will be analyzed, where an episode of sea breeze with an omega configuration occurred with winds from the west that favoured the absence of important cloud accumulations on the island, this is due to the fact that these strong winds prevent the vertical ascent of the air mass to form these accumulations, so there was no precipitation in any meteorological stations for this day.

3.2.1. Meteorological stations

From the six stations of Fuerteventura, the airport station (C249I) and the Puerto Gran Tarajal station (C239N) were chosen for this day because they showed the presence of the sea breeze in a better way. A station from the interior of the island was not been chosen because the sea breeze did not reach these stations. (Fig. 14).

At the airport station (Fig. 14a) it was possible to observe a generally weak wind during the day. It should be noted that during the night the wind direction was variable, and, during the day, a constant SE wind can be seen between 1000-1900 UTC. The minimum temperature was 17º C and took place between 0600-0700 UTC, and the maximum was 22º C, recorded at 1400 UTC. The flow turned to a maritime component (SE component) as in March event (red box).

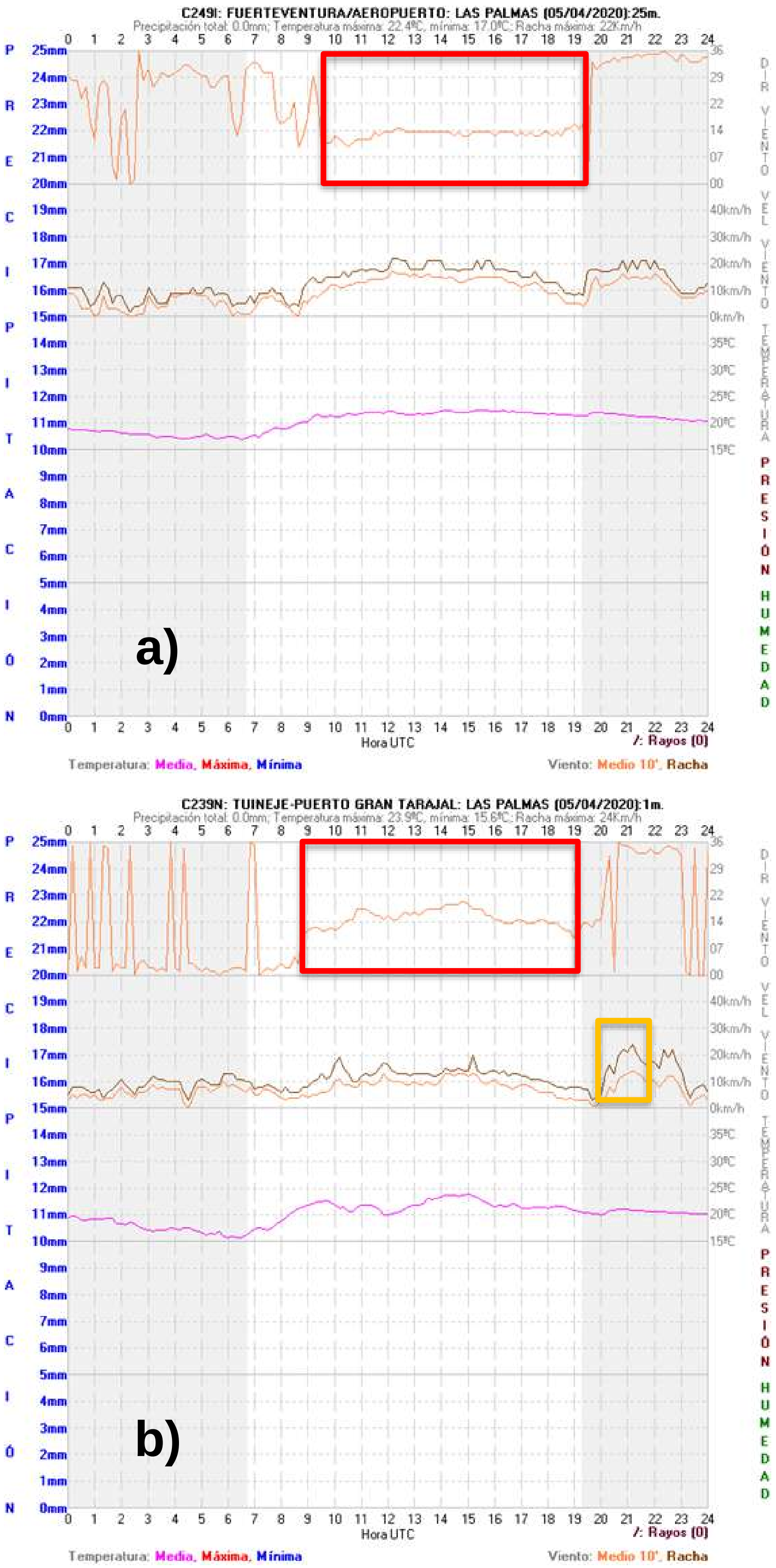

Fig. 14 Same as in Fig. 8, but for 5 April 2020. **a)** Airport station **b)** Puerto Gran Tarajal station (Source: AEMET).

In the Puerto Gran Tarajal station (Fig. 14b), a generally weak wind can be observed during the day. It should be noted that during the night the wind direction was not very variable, being of N component, and during the day a wind direction of SE component can be seen (red box). In addition, a maximum gust of 24 km/h at 2100 UTC standed out, as shown in the orange box. The minimum temperature was 16º C and was recorded between 0600-0700 UTC, and the maximum was 24º C at 1500 UTC.

As in the situation on 18 March 2017, the six AEMET stations have been studied and two of them have been analyzed and exposed for the situation on 5 April 2020. Similarly, in order to present the situation in the other stations, the most important data from each station have been collected for this day (Table 2).

Table 2 Same as in Table 1, but for 5 April 2020.

Station	**Name**	**Height (m)**	**TN (°C)**	**TM (°C)**	**Prec (mm)**	**RM (km/h)**	**Wind strength**	**Breeze**
C259X	**La Oliva-Pto**	**6**	**18.1**	**23.0**	**0.0**	**34**	**Weak**	**No**
C258K	**La Oliva-Ctra del Cotillo**	**217**	**15.3**	**25.0**	**0.0**	**36**	**Weak**	**No**
C249I	**Aeropuerto**	**25**	**17.0**	**23.4**	**0.0**	**22**	**Weak**	**Yes**
C248E	**Antigua-El Carbón**	**252**	**16.4**	**23.9**	**0.0**	**37**	**Weak**	**No**
C239N	**Tuineje-Pto**	**1**	**15.6**	**23.9**	**0.0**	**24**	**Weak**	**Yes**
C229J	**Pájara-Pto**	**15**	**18.1**	**25.1**	**0.0**	**34**	**Weak**	**Yes**

3.2.2. HRES-IFS Model

As in the previous situation, the HRES-IFS model was also used to study the synoptic environment and a simulated sounding on the island of Fuerteventura for April 5th, 2020.

Synoptic environment

In the synoptic environment for 5 April 2020, a geopotential omega configuration centered on the north of France and a zonal flow with westerly winds at high altitude over the Canary Islands were observed in the temperature map at 500 hPa (Fig. 15a). Moreover, it can be seen in the pressure map at sea level that the Canary Islands were inside a barometric swamp and, in the vicinity, an anti-cyclone with a maximum pressure of 1020 hPa centered in the Atlantic Ocean to the west of the islands and a low with a minimum of 1016 hPa centered on the African continent (Fig. 15b). The Canary Islands were therefore affected by a northward flow on the surface.

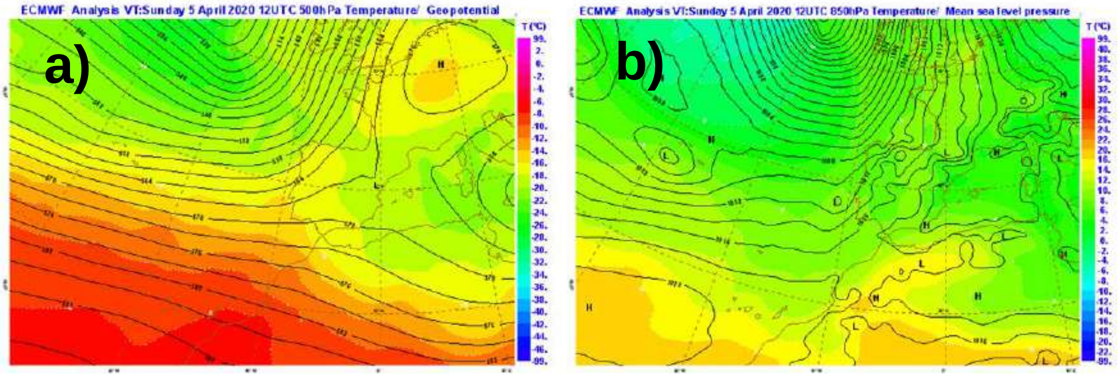

Fig. 15 Same as in Fig. 9, but for 5 April 2020, 1200 UTC (Source: AEMET).

Sounding

A simulated sounding of the HRES-IFS model with the same resolution as in the previous situation was used to observe the instability present on the island of Fuerteventura for 5 April 2020 (Fig. 16).

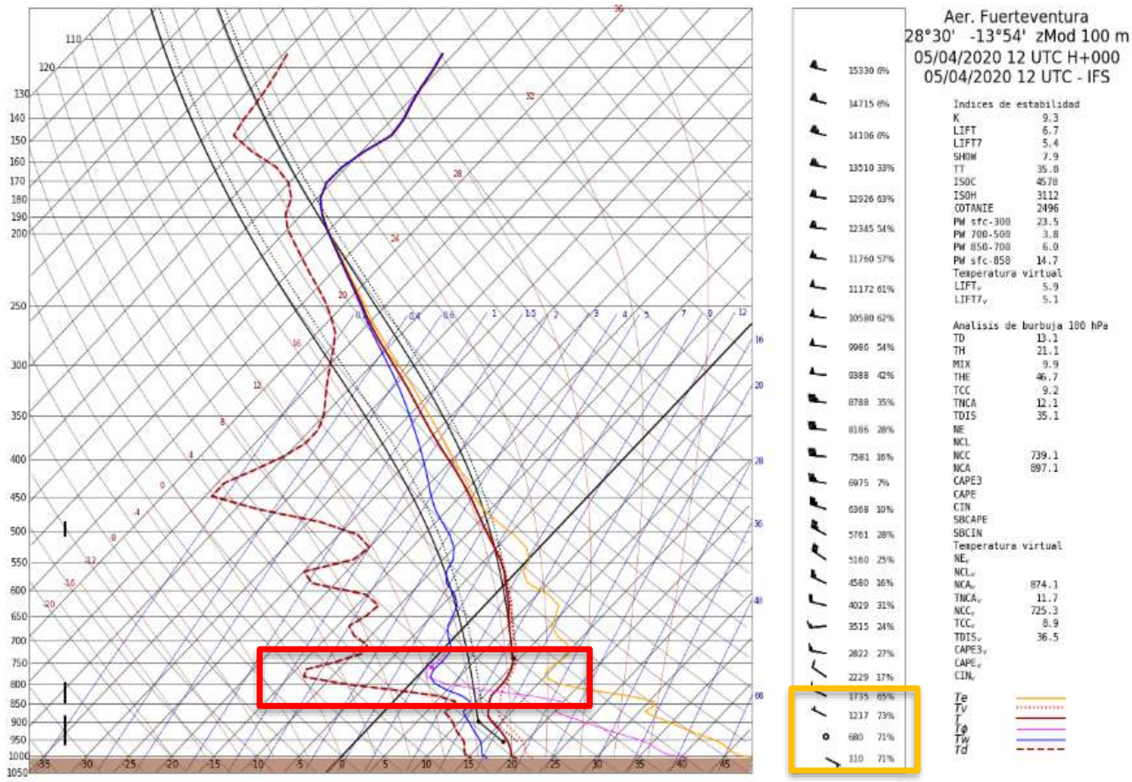

Fig. 16 Same as in Fig. 10, but for 5 April 2020, 1200 UTC (Source: AEMET).

The simulated sounding on the island of Fuerteventura at 1200 UTC for April 5th 2020 showed that the inversion of the trade winds was strong, this was due to the fact that a subsidence inversion occured at an altitude between 800-850 hPa as shown in the red box. A change in wind direction can be seen at 680 m as it moved from ESE to WSW (orange box). There may be clouds at an altitude between 800-900 hPa as T and Td approach and the air is more humid. In addition, a value of <15 in the K index is observed in the stability indices, indicating that there is no possibility of a storm (0%), a positive value in the LIFT index favours stability and a value below 44 in the TT index indicates the low probability of a severe local storm (AMS 2012).

3.2.3. WRF Model

The same tool has been used to create two forecasts showing the evolution of different variables on the island and to create vertical sections W-E across the airport station and which are also perpendicular to the coast (Fig. 5b).

WRF forecasts

The same several described in the previous situation have been studied. Where an image is shown with wind at 10 m with temperature at 2 m (Fig. 17a) and another showing wind speed at 10 m with wind module (Fig. 17b). For more detail, it was observed in the island of Fuerteventura for the day 5 April 2020 that between 1300-1800 UTC a convergence is shown in the interior of the island as shown in the direction of the wind at 1300 UTC (Fig. 17a) and the front of the breeze was also shown and it was observed that this did not penetrate so much in the island as in the case of 18 March 2017, having its maximum advance also at 1300 UTC (Fig. 17b). Also, it can be seen the small SBF in red box (Fig. 17b).

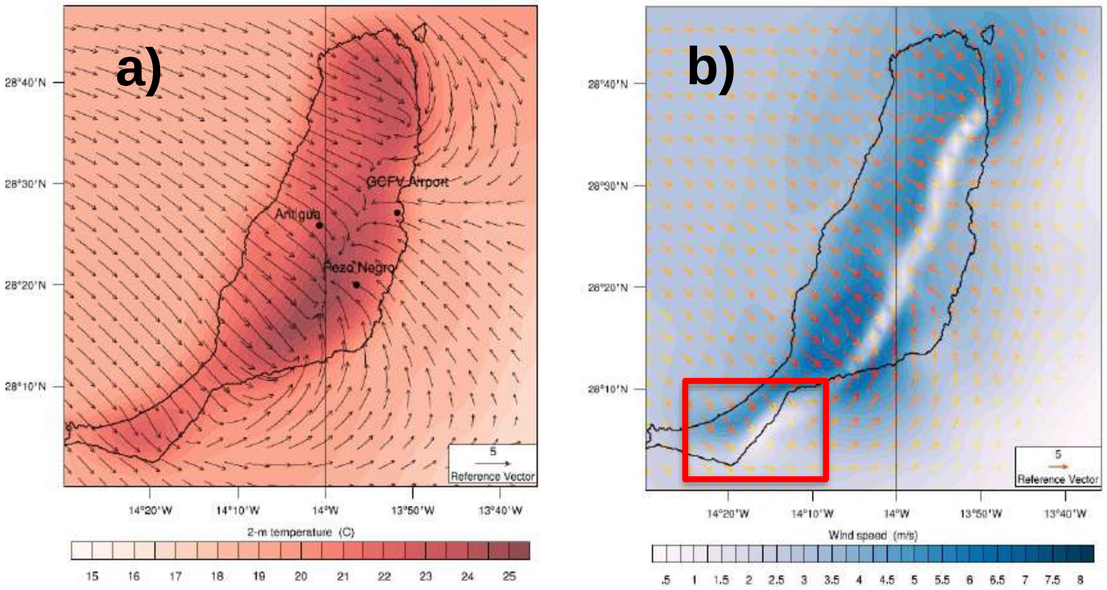

Fig. 17 Same as in Fig. 11, but for 5 April 2020, 1300 UTC.

Cross-sections

The WRF model has been used to observe the vertical cross sections as the March event but for 5 April 2020 (Fig. 18).

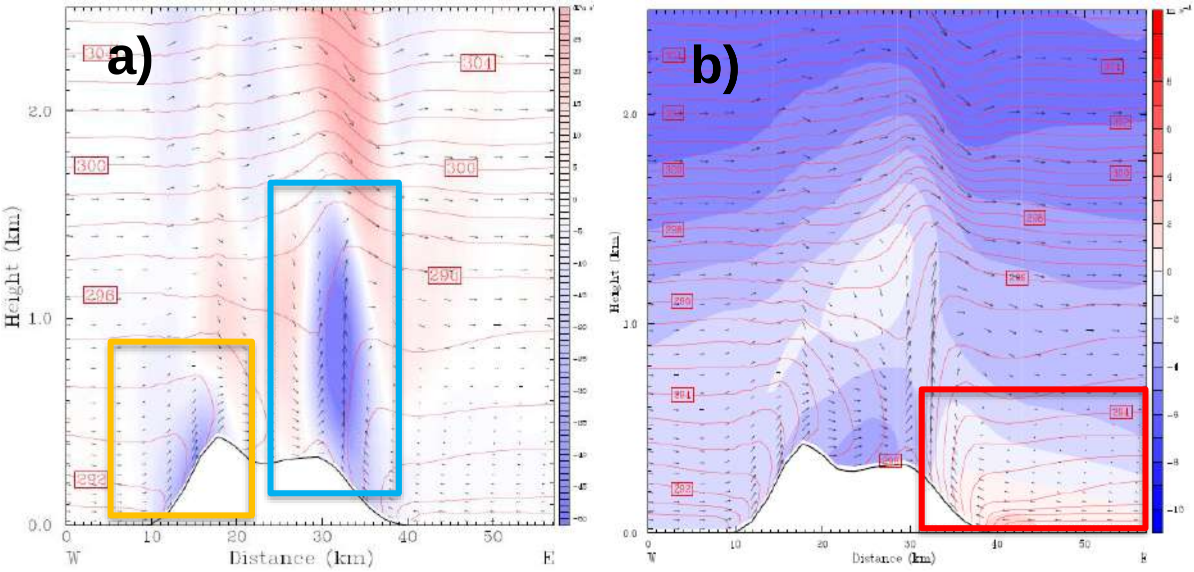

Fig. 18 Same as in Fig. 12, but for 5 April 2020, 1300 UTC.

For the situation in April 2020, something similar to the one in March was presented, but of a lesser magnitude since there was a vertical speed but it only reaches 1.5 km in height as shown in the blue box (Fig. 18a). The cause of this variation with the previous situation was the absence of cold core in height, which prevent the development of the vertical speeds observed in (Fig. 18a). Furthermore, the cell of the sea breeze (red box) does not penetrate as much into the island as in the previous case, reaching approximately 7 km inland (Fig. 18b). In this case, a sea breeze can also be observed on the west face of the island due to the vertical speed observed in the orange box (Fig. 18a)(Cana et al. 2020).

3.2.4. Satellite images

In order to observe the cloudiness present on the island, as in the previous case, satellite images of the MSG with the HRVIS channel were used for 5 April 2020. A continuous line of clouds can be seen parallel to the east coast of the island of Fuerteventura as shown in the red box (Fig. 19). Furthermore, this cloud band was not as developed as in the March situation, this was due to all that has been commented previously.

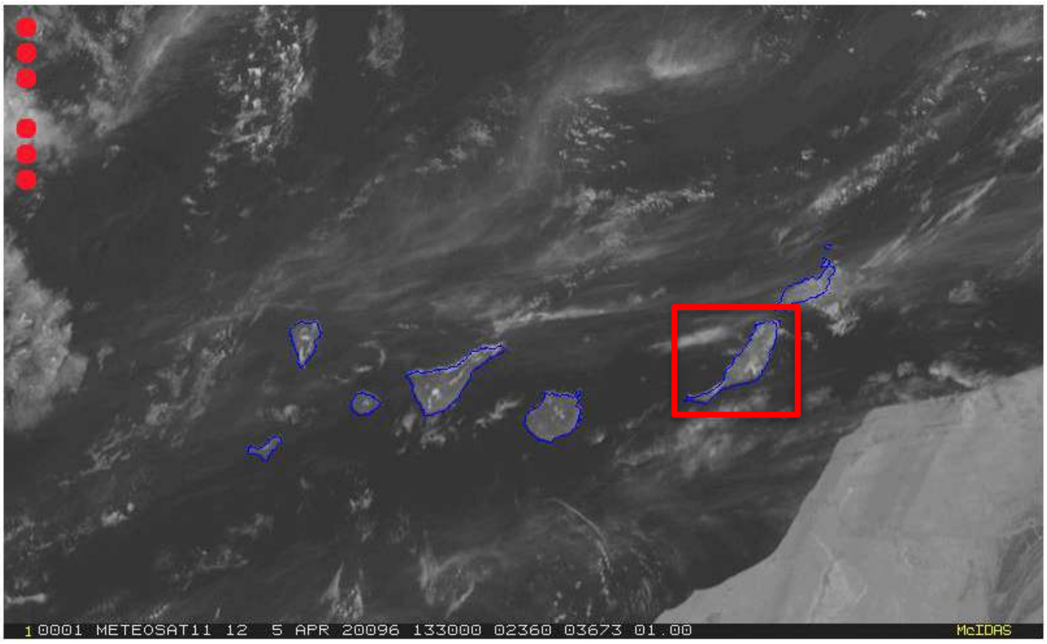

Fig. 19 Same as in Fig. 13, but for 5 April 2020, 1330 UTC (Source: AEMET).

4. Conceptual model

Throughout this work, a definition of sea breeze, the fundamental characteristics it possesses and the physical method behind this phenomenon have been shown and a selection of valid maps and simulations have been exposed to be able to describe, in terms of the extension and life cycle, a conceptual model of the sea breezes on the Fuerteventura island, according to the points exposed in the methodology. In this model, a front of the breeze will be shown with a vertical dimension between 500-700 m but which, in the total dimension of the breeze, will reach 2 km due to the existence of the return current.

The following diagrams show, on the one hand, the conceptual model differentiating the vertical processes (Fig. 20a) from the horizontal ones (Fig. 20b) using the dimensions of the vertical cross sections across the airport station used in the results section and, on the other hand, the general conceptual model of the island of Fuerteventura (Fig. 21).

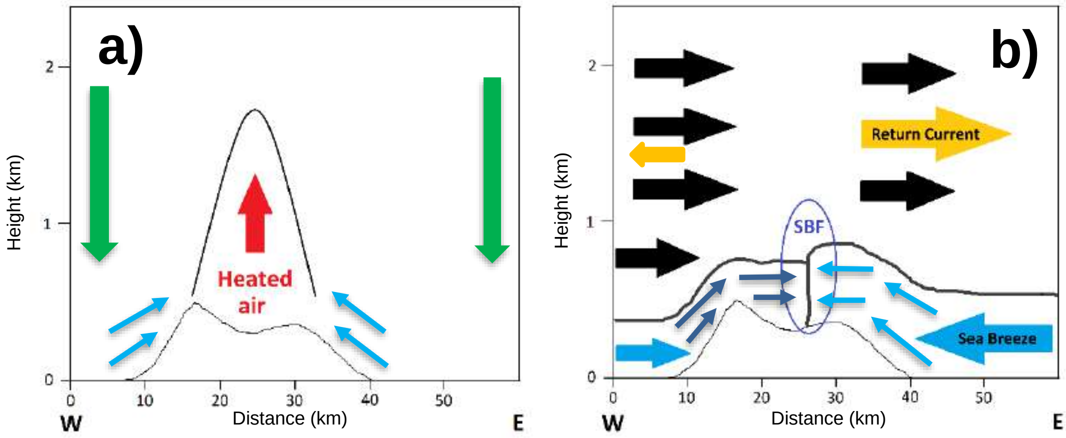

Fig. 20 Conceptual model for sea breeze development in Fuerteventura. This scheme shows the vertical processes **(a)** and the horizonal processes **(b).**

In these figures it can be seen the typical circulation of a sea breeze applied to the island of Fuerteventura, where you can see the arrows of different colours that serve to identify each air movement, so they indicate only the variable direction of the wind. In the figure on the left that, due to the temperature difference between land and ocean explained above in a theorical way, a pressure gradient is formed that causes the hot air above the island to rise and the cooler air above the ocean occupies the space left by that hot air. For this figure, the red arrow indicates the vertical movement in the central zone on the island due to the rise of hot air. Instead, the small blue arrows indicate the vertical displacement of the sea breezes (cold front) moving along both sides of the island. In addition, the green arrows represent a current at the top of the two sea breeze cells that returns the air to the ocean by subsidence (Fig. 20a).

The diagram on the right shows black arrows that indicate the general flow of the wind with W component. The light blue arrows show the direction in which the sea breezes travel from the ocean to the central areas of the island through the two faces. It should be noted that dark blue arrows are shown in the west face breeze, because the winds of the general flow (black) are added to those of the breeze (light blue). And, the yellow arrows show the return current of each breeze circulation, where one is represented larger than the other. This is because the return current in the circulation of the east face is in favour of the general flow, while the return current of the west face is against and, therefore, it cannot be identified as well as the previous one. It should be noted that the convergence at the low levels is strong due to the collision of winds from opposite directions, right where the SBF is (blue circle).

A general conceptual model of the sea breezes in Fuerteventura is shown (Fig. 21). The circulation of the sea breeze at the height of the airport explained above is exposed, but with the difference that, in this case, subsidence is shown (green arrow), the phenomenon that returns the air to the surface of the ocean to close the cycle of the sea breeze. This is because the subsidence could not be identified with the scale of the previous graphs, and the other circulation is on Morro Jable (blue box). These two circulations are shown because two fronts of sea breezes are formed; these can be observed in more detail in Fig. 22. It should be noted that throughout the SBF, as it advances inland. The cumulus cloudiness is increasing, which can be identified by satellite images as a continuous line of clouds parallel to the coast called sea breeze cloudiness. In Fig. 22 shows a map of Fuerteventura, where you can see in more detail the two fronts (black lines) at their maximum advance around 1300 UTC, during a sea breeze event, this explains the two circulations of breezes shown in Fig. 21. Furthermore, the sea breeze cloudiness can be formed along the two fronts.

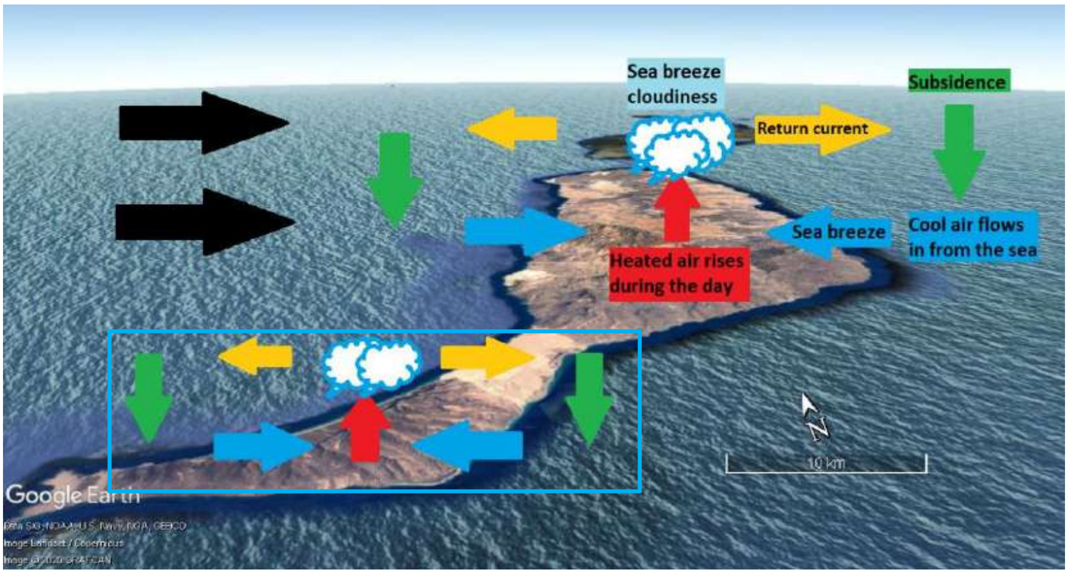

Fig. 21 General conceptual model of sea breeze development in Fuerteventura. Modified image of Google Earth Pro.

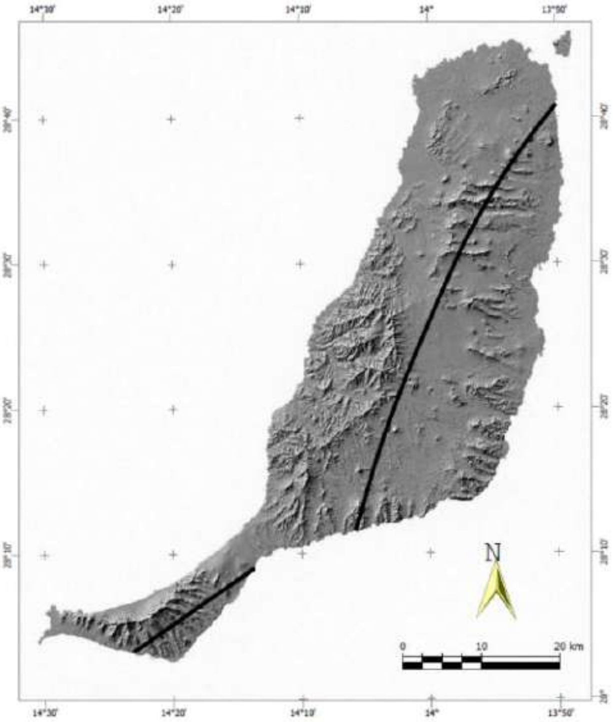

Fig. 22 Fuerteventura Map showing the two SBFs that occur during a sea breeze event.

The key meteorological field that must be analysed to identify a sea breeze situation is wind direction because it has been observed that the sea breeze of the east face evolves when the wind has maritime component, this occurs when the trade winds are not present. Whether these winds occur or not depends directly on the synoptic situation of that day. Therefore, if the islands are within a barometric swamp, the synoptic wind (trade winds) will be weak, and the sea breeze can develop.

The initial time condition that produces a sea breeze situation on the Fuerteventura island is the change of wind in the direction opposite to the main flow, in this case, the change is from NW to SE, where this wind of SE component intensifies and creates the SBF. This cold front begins to advance parallel to the east coast of the island. And the second weather condition that is observed is the increase in cloudiness with a cumulus-type development, a structure that is identified with satellite images is the sea breeze cloudiness, a phenomenon explained throughout the work. Depending on the synoptic pattern that occurs, there may or may not be rainfall on the island. In this study, an example of a situation of breezes with heavy rainfall (March event) and another situation where there was no precipitation, although cumulus-type cloudiness was formed (April event).

In this study, it has been observed that a minimum temperature difference of 2º C between land and ocean is necessary for a breeze to be produced, which will mean a decrease in pressure on the coast and an increase in the sea, as a result, there is the movement of the air over the ocean towards the island. The minimum temperature difference is about 2º C because the temperature in the airport station was compared to the mean SST (sea-surface temperature) in the east coast for 5 April 2020. In the airport station had 21º C approximately at 1000 UTC and the SST was 19.2º C in the waters near to airport station. The SST data are taken from the NASA EOSDIS Worldview as a base layer for the model.

5. Discussion

The results obtained from the meteorological stations of Fuerteventura have helped to describe the extension (distribution) and life cycle of the sea breeze. These data from the stations are aimed at studying, in detail, the sea breeze that forms on the east coast of the island. Later, the sea breeze that forms on the west coast could be appreciated through the simulated images and cross sections. This is because the main flow is traveling in the same direction as this breeze. In addition, it was observed, in the simulated images, that two fronts were formed on the island, a larger main over a large part of the island, which is clearly identified and then, another front much smaller, forms in the Morro Jable area. This small front is shown in the general model as another breeze circulation in that area. With the simulated soundings it was possible to observe the instability of the island, determining the possibility of precipitation, if the inversion of the trade winds was strong or weak, useful information to explain the development of cloudiness on the island. With the satellite images, it was possible to identify the sea breeze cloudiness and the cumulus-type development cloudiness that could cause rains on the island.

The synoptic environment has been a key tool in determining whether there is a breeze in the area. In a particular way, two synoptic situations have been observed in this work, one with a low altitude and another with westerly winds, which have shown to have clear differences that determined the climatic conditions on the island. Although they also have similarities that are seen in all episodes of breezes and are the change in wind direction to be perpendicular to the coast and the increase in cloud cover.

6. Conclusions

- In this study, the aim to create the conceptual model of sea breezes on the island of Fuerteventura has been achieved. The model has been exposed, differentiating the vertical from the horizontal processes, and a general model of the breezes on the island has also been shown in a schematic way.
- There must be a change in wind direction from a NE component (trade winds) to a maritime component (SE component).
- A minimum temperature difference of 2º C is necessary for a sea breeze to be produced in Fuerteventura.
- The sea breeze begins between 0900-1000 UTC with daytime warming, has a maximum advance around 1300 UTC, retreats from this time and disappears completely around 1900 UTC.
- Two fronts are displayed on the island, a principal one in the mayor part of the island and another, much smaller, in the Morro Jable location. Moreover, there is a leeward sea breeze circulation and a windward breeze circulation occurring at the same time in each front, as it has been observed in the conceptual model.

It should be noted that the model shows the fundamental direction of winds that will always be detected in a sea breeze situation on Fuerteventura island. But it can be greatly improved if the temperature and pressure variables are observed in detail in order to add them to the conceptual model. Furthermore, it would be interesting to be able to describe a more specific conceptual model for each synoptic situation that favours the evolution of the sea breeze, with the aim of having the best prediction on this island.

7. References

AEMET (2015) Manual de uso de términos meteorológicos. Agencia Estatal Meteorol. 36

AEMET (2018) Climatología Aeronáutica. Catálogo Publicaciones la Adm. Gen. del Estado 115

AEMET (2020a) Escalas meteorológicas. In: Meteoglosario Vis. https://meteoglosario.aemet.es/es/termino/191_escalas-meteorologicas

AEMET (2020b) Modelo determinista del ECMWF-CEPPM (HRES-IFS). In: Meteoglosario Vis. https://meteoglosario.aemet.es/es/termino/1009_modelo-determinista-del-ecmwf-ceppm-hres-ifs

AEMET (2020c) Inestabilidad atmosférica. In: Meteoglosario Vis. https://meteoglosario.aemet.es/es/termino/1016_inestabilidad-atmosferica

AMS (2012) Stability Index. In: Meteorol. Gloss. http://glossary.ametsoc.org/wiki/Stability_index

Cana L, Grisolía-Santos D, Hernández-Guerra A (2020) A Numerical Study of a Sea Breeze at Fuerteventura Island, Canary Islands, Spain. Boundary-Layer Meteorol 175:277–296. https://doi.org/10.1007/s10546-020-00506-z

Carrillo J, Guerra JC, Cuevas E, Barrancos J (2016) Characterization of the Marine Boundary Layer and the Trade-Wind Inversion over the Sub-tropical North Atlantic. Boundary-Layer Meteorol 158:311–330. https://doi.org/10.1007/s10546-015-0081-1

Crosman ET, Horel JD (2010) Sea and Lake Breezes: A Review of Numerical Studies. Boundary-Layer Meteorol. 137:1–29

Dorta Antequera P (1996) Las inversiones térmicas en Canarias. Investig Geográficas 109–124. https://doi.org/10.14198/ingeo1996.15.01

EUMeTrain (2020) Sea Breeze: Meteorological Physical Background. In: eumetrain.org. http://www.eumetrain.org/satmanu/CMs/SB/navmenu.php?page=2.0.0

EUMETSAT (2020) INTRODUCTION TO CONCEPTUAL MODELS. https://eumetsat.int/website/home/Data/Training/TrainingLibrary/DAT_2043086.html

Ferdiansyah MR, Inagaki A, Kanda M (2020) Detection of sea-breeze inland penetration in the coastal-urban region using geostationary satellite images. Urban Clim 31:100586. https://doi.org/10.1016/j.uclim.2020.100586

García Couto MA (2012) Atlas climático de los archipiélagos de Canarias, Madeira y Azores. Aemet 79

Holton JR, Hakim GJ (2004) An introduction to dynamic meteorology: Fourth edition. Elsevier Acad Press 9780123848:1–532. https://doi.org/10.1016/C2009-0-63394-8

Lin Y-L (2007) Mesoscale Dynamics. Cambridge Univ Press 1–12

Miller STK, Keim BD, Talbot RW, Mao H (2003) Sea breeze: Structure, forecasting, and impacts. Rev. Geophys. 41

Orlanski I (1975) A Rational Subdivision of Scales for Atmosferic Processes. Bull Am Meteorol Soc 56:527

Suárez Molina D, Fernández-González S, Suárez González JC, Oliver A (2020) Analysis of sounding derived parameters and application to severe weather events in the Canary Islands. Atmos Res 237:104865. https://doi.org/10.1016/j.atmosres.2020.104865

Torres CJ, Cuevas E, Guerra JC, et al (2001) Caracterización de las masas de aire en la región subtropical sobre Canarias. Inst Nac Meteorol 2–7

ZAMG (2020) CONCEPTUAL MODELS - DEFINITION. http://rammb.cira.colostate.edu/wmovl/VRL/Tutorials/SatManu-eumetsat/SatManu/Basic/CM/CM.htm